1521-009X/45/3/316–324$25.00
Drug Metabolism and Disposition

http://dx.doi.org/10.1124/dmd.116.073239
Drug Metab Dispos 45:316–324, March 2017

Stereoselective Pharmacokinetics and Chiral Inversion of Ibuprofen in Adjuvant-induced Arthritic Rats

Hiroyuki Ikuta, Atsushi Kawase, and Masahiro Iwaki

Department of Pharmacy, Faculty of Pharmacy, Kindai University, Higashi-osaka, Osaka, Japan

Received August 23, 2016; accepted December 1, 2016

ABSTRACT

2-Arylpropionic acid (2-APA) nonsteroidal anti-inflammatory drugs are commonly used in racemic mixtures (*rac*) for clinical use. 2-APA undergoes unidirectional chiral inversion of the in vivo inactive *R*-enantiomer to the active *S*-enantiomer. Inflammation causes the reduction of metabolic activities of drug-metabolizing enzymes such as cytochrome P450 (P450) and UDP-glucuronosyltransferase. However, it is unclear whether inflammation affects the stereoselective pharmacokinetics and chiral inversion of 2-APA such as ibuprofen (IB). We examined the effects of inflammation on the pharmacokinetics of *R*-IB and *S*-IB after intravenous administration of *rac*-IB, *R*-IB, and *S*-IB to adjuvant-induced arthritic (AA) rats, an animal model of inflammation. The plasma protein binding of *rac*-IB, glucuronidation activities for *R*-IB and *S*-IB, and P450 contents of liver microsomes in AA rats were determined. Total clearance (CL_{tot}) of IB significantly increased in AA rats, although the glucuronidation activities for IB, and P450 contents of liver microsomes decreased in AA rats. We presumed that the increased CL_{tot} of IB in AA rats was caused by the elevated plasma unbound fraction of IB due to decreased plasma albumin levels in AA rats. Notably, CL_{tot} of *R*-IB but not *S*-IB significantly increased in AA rats after intravenous administration of *rac*-IB. These results suggested that AA could affect drug efficacies after stereoselective changes in the pharmacokinetics of *R*-IB and *S*-IB.

Introduction

The 2-arylpropionic acid (2-APA) nonsteroidal anti-inflammatory drugs, with the exception of naproxen, are commonly used in racemic mixtures (*rac*) for clinical use. The *S*-enantiomer of 2-APA confers therapeutic effects via prostaglandin synthesis inhibition and causes adverse effects such as gastrointestinal irritation (Brune et al., 1992). 2-APA undergoes unidirectional chiral inversion of the in vivo inactive *R*-enantiomer to the active *S*-enantiomer, which appears to be species and compound dependent (Caldwell et al., 1988; Baillie et al., 1989; Knihinicki et al., 1989; Chen et al., 1990; Müller et al., 1990; Ahn et al., 1991; Chen et al., 1991; Rudy et al., 1991). Stereoselective pharmacokinetic studies of 2-APA have been performed in rodents and humans (Abas and Meffin, 1987; Foster et al., 1988; Jamali et al., 1988; Pedrazzini et al., 1988; Jamali and Brocks, 1990; Brocks and Jamali, 1994; Davies, 1995; Castro et al., 2001).

The liver is susceptible to inflammation such as viral and drug-induced hepatitis and is the primary organ for metabolism of xenobiotics and endogenous substrates. We previously demonstrated alterations in expression and activity of drug-metabolizing enzymes and transporters in inflammation using mice with collagen-induced arthritis (Kawase et al., 2007) and rats with adjuvant-induced arthritis (AA) (Uno et al., 2007,2009).

This work was supported by the "Antiaging" Project for Private Universities, with a matching fund subsidy from the Japanese Ministry of Education, Culture, Sports, Science and Technology (MEXT); the MEXT-Supported Program for the Strategic Research Foundation at Private Universities 2014-2018 [Grant S1411037].

dx.doi.org/10.1124/dmd.116.073239.

AA rats have been used as a model of rheumatoid arthritis for the development of anti-inflammatory medicines because they exhibit systemic inflammatory disease with changes to bone and cartilage similar to those observed in humans with rheumatoid arthritis (Williams, 1992). Increases in inflammatory markers such as lactate dehydrogenase, aspartate aminotransferase, alkaline phosphatase, and α_1-acid glycoprotein were observed in the serum of AA rats (Kawase et al., 2013). Several reports have shown that the elimination of propranolol (Walker et al., 1986; Piquette-Miller and Jamali, 1995), acebutolol (Piquette-Miller and Jamali, 1992), and cyclosporine (Pollock et al., 1989) from blood is delayed in AA rats. The alterations in drug pharmacokinetics in AA rats are possibly attributed to changes in plasma binding to albumin and impaired metabolism by metabolic enzymes such as cytochrome P450 (P450) and UDP-glucuronosyltransferase (UGT). Most 2-APA drugs are highly bound to plasma albumin and are mainly eliminated by hepatic metabolism. Meunier and Verbeeck (1999a) reported the stereoselective glucuronidation of ketoprofen in AA rats. They showed that AA rats exhibit significant impairment in the in vivo glucuronidation of ketoprofen. Consequently, the disposition of drugs that undergo low hepatic extraction can be especially affected by pathophysiological changes in arthritis. We demonstrated that the total clearance (CL_{tot}) of flurbiprofen enhanced owing to a remarkable decrease in protein binding despite impaired intrinsic hepatic clearance (CL_{int}) (Nagao et al., 2003).

However, there is little information regarding the pharmacokinetics of chiral inversion of 2-APA in arthritis, despite 2-APA being widely administered to patients suffering from arthritis. Ibuprofen (IB) as a model compound of 2-APA undergoes unidirectional chiral inversion of

ABBREVIATIONS: 2-APA, 2-arylpropionic acid; AA, adjuvant-induced arthritis; ACS, acyl-coenzyme A synthetase; APCE, 2-aryl propionyl-coenzyme A epimerase; AUC, area under the plasma concentration-time curve; CL_{int}, intrinsic hepatic clearance; CL_{MET}, metabolic clearance; CL_{RS}, chiral inversion clearance; CL_{tot}, total clearance; f_u, unbound fractions; HPLC, high-performance liquid chromatography; IB, ibuprofen; IBG, ibuprofen glucuronide; ID, inside diameter; k_{RS}, inversion rate constants; OD, outside diameter; P450, cytochrome P450; rac, racemic mixtures; $T_{1/2inv}$, half-life for inversion; UGT, UDP-glucuronosyltransferase; V_1, central compartment; V_2, peripheral compartment; Vd_{ss}, distribution volumes at steady state.

the inactive *R*-enantiomer to the active *S*-enantiomer in rats (Kaiser et al., 1976). We previously demonstrated that the intrinsic chiral inversion rate constant of IB and the metabolic degradation rate constants decreased in AA rats compared with those of control rats in freshly isolated rat hepatocytes (Uno et al., 2008). This in vivo study was carried out to clarify the effects of AA inflammation on the stereoselective pharmacokinetics of *R*-IB and *S*-IB and chiral inversion of IB after intravenous administration to rats.

Materials and Methods

Ethical Approval of the Study Protocol. The study protocol was approved by the Committee for the Care and Use of Laboratory Animals of the Faculty of Pharmacy of Kindai University (Osaka, Japan).

Compounds and Reagents. *Rac*-IB was purchased from Wako Pure Chemicals (Osaka, Japan). *R*-IB and *S*-IB were purchased from Cayman Chemical Company (Ann Arbor, MI) and Tokyo Kasei (Tokyo, Japan), respectively. Naproxen and etodolac, internal standards for high-performance liquid chromatography (HPLC), were purchased from Sigma Aldrich (St. Louis, MO) and Nippon Shinyaku (Kyoto, Japan), respectively. Rabbit polyclonal anti-acyl-coenzyme A synthetase (ACS)1 antibody (Bioss Antibodies, Woburn, MA), rabbit polyclonal anti-2-aryl propionyl-coenzyme A epimerase (APCE) antibody (Cell Signaling Technology, Danvers, MA), and mouse monoclonal anti-β-actin (Acris Antibodies, Herford, Germany). All other chemicals and solvents were of the best purity commercially available or of HPLC grade.

Preparation of AA Rats. Female Sprague-Dawley rats (7 weeks old) weighing 150–170 g were purchased from Japan SLC (Shizuoka, Japan). The animals were housed in a temperature-controlled room with free access to standard laboratory food and water. AA rats were prepared according to a previously reported procedure (Kawase et al., 2014). Briefly, 1 mg heat-killed *Mycobacterium butyricum* was subcutaneously injected into the right hind footpad and tail base of rats (Difco Laboratories, Detroit, MI) as an adjuvant suspended in Bayol F oil (10 mg/ml). Hind paw volumes were measured using a liquid plethysmometer. Animals that exhibited severe inflammation at local and systemic sites at 21 days (chronic phase) after injection of the adjuvant were studied.

Animal Experiments. On the day before drug administration, a cannula (silicone tubing; 0.5 mm inside diameter [ID], 1.0 mm outside diameter [OD]) was implanted in the right jugular vein under pentobarbital anesthesia (40 mg/kg, intraperitoneally). On day 21 after AA induction, the bile ducts of the animals were cannulated with polyethylene tubing (PE-10; 0.28 mm ID, 0.61 mm OD) to avoid possible enterohepatic circulation of IB (Dietzel et al., 1990). Animals received intravenous administration of either *rac*-IB (20 mg/kg) or each IB enantiomer (10 mg/kg) through the jugular vein cannula, followed by 0.3 ml of sterile heparinized saline to flush the tubing. Blood samples were collected 1, 5, 10, 20, 30, 45, 60, 90, and 120 minutes after administration and were centrifuged for 10 minutes at 3000 g. Because of the instability of acyl glucuronides at physiologic pH, plasma was transferred to a tube containing 5 μl 17% phosphoric acid. The plasma was immediately frozen on dry ice and stored at –80°C until analysis.

Protein Binding Study. In vitro filtrated unbound IB at a total concentration of 50 μg/ml was determined by ultrafiltration (MINICENT-10, Tosoh, Tokyo, Japan) of plasma samples from control and AA rats without IB treatment to evaluate the plasma protein binding of IB. In vivo plasma protein binding in control and AA rats was also measured after intravenous administration of *rac*-IB (20 mg/kg). Preliminary studies indicated that IB did not bind to the ultrafiltration device. Plasma albumin and total protein concentrations were determined by an automatic analytical device (Olympus AU5200, Olympus, Tokyo, Japan).

Glucuronidation Activities and P450 Contents in Liver Microsomes. The UGT activities in rat liver microsomes for IB enantiomers were determined. After incubating 1 mM IB for 10 minutes in the microsomal suspension in 0.1 M Tris-HCl buffer (pH 7.4) including 1 mg/ml microsome, 10 mM $MgCl_2$, 0.2% Triton X-100, 2 mM phenyl methyl sulfonyl fluoride, 20 mM 1,4-saccharolactone, and 10 mM UDP-glucuronic acid, the concentrations of IB glucuronide (IBG) formed were stereoselectively determined by HPLC. P450 contents in rat liver microsomes were determined by the method described by Omura and Sato (1964).

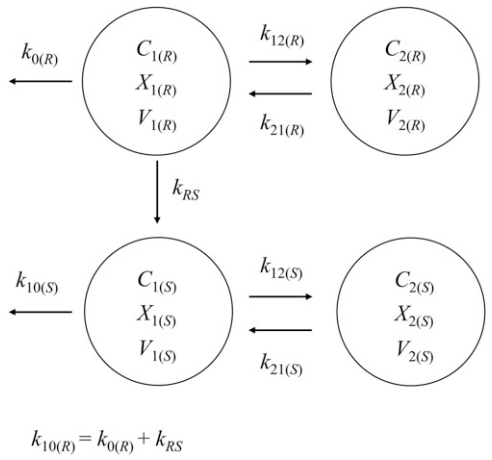

Fig. 1. A pharmacokinetic model with unidirectional inversion from *R*-IB to *S*-IB.

Sample Preparation for HPLC Analysis. Naproxen (50 μl) in methanol (1 μg/ml) was added as an internal standard to mixtures of 100 μl plasma and 400 μl acetic acid (pH 2.5). After the addition of 2 ml ethyl acetate, the mixture was shaken for 10 minutes and centrifuged at 2000 *g* for 5 minutes. The organic layer was transferred to another clean tube and evaporated to dryness using a centrifugal evaporator (Tokyo Rikakikai, Tokyo, Japan) at 35°C. The 20-μl residue dissolved in 100 μl of mobile phase was injected into the HPLC system. For bile samples, 50 μl of etodolac in methanol (5 μg/ml) as an internal standard and 100 μl of methanol were added to bile diluted 10 times with purified water. The mixture was vortexed for 30 seconds and centrifuged at 2000 *g* for 5 minutes, and the 20 μl supernatant was directly injected into the HPLC system.

HPLC Conditions. HPLC analysis was performed using a conventional ODS column (Cosmosil 5C18-AR-II, 4.6 × 250 mm, 5 μm, Nacalai Tesque, Kyoto, Japan) for *rac*-IB and a chiral column (Chiral OJ-R, 4.6 × 150 mm, 5 μm, Daicel Chemical, Tokyo, Japan) for *R*-IB, *S*-IB, *R*-IBG, and *S*-IBG using a Shimadzu HPLC system equipped with an ultraviolet detector (220 nm for IB assay; 232 nm for IBG assay). The mobile phases [0.2 M phosphate buffer, pH 2.0/acetonitrile (67.5:32.5, v/v) for IB assay, and 0.05 M phosphate buffer including 2 mM tetra-*n*-butylammonium hydrogen sulfate, pH 5.5/acetonitrile (65:35, v/v) for IBG] were pumped at a flow rate of 1 ml/min.

Pharmacokinetic Analysis. Plasma concentration data for IB were fitted to the mass balance equation for a conventional two-compartment open model with unidirectional inversion from *R*-IB to *S*-IB (Fig. 1) (Knihinicki et al., 1990). We tried to one- and two-compartment model including chiral inversion. The Akaike's information criterion of two-compartment model was smaller than that

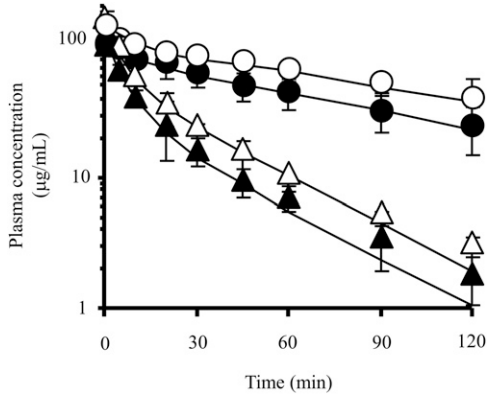

Fig. 2. Plasma concentration-time profiles of IB enantiomers after intravenous administration of *rac*-IB (20 mg/kg) in control and AA rats.△, *R*-IB; ○, *S*-IB in control rat; ▲, *R*-IB; ●, *S*-IB in AA rats. Solid lines represent the fitting curves using the pharmacokinetic model shown in Fig. 1. Results are expressed as the mean ± S.D. (n = 3).

TABLE 1

Noncompartmental pharmacokinetic parameters of each enantiomer after intravenous administration of *rac*-IB

Results are expressed as the mean ± SD (n = 3).

Parameter	Control		AA	
	R-IB	*S*-IB	*R*-IB	*S*-IB
$T_{1/2}$ (min)	35.7 ± 6.8	89.5 ± 37.1	30.7 ± 6.5	69.0 ± 17.0[b]
CL_{tot} (ml/min/kg)	3.70 ± 0.14	0.80 ± 0.27[b]	5.40 ± 0.71[a]	1.20 ± 0.31[b]
MRT (min)	32.7 ± 3.9	127 ± 51.9[b]	30.3 ± 5.7	97.5 ± 29.5[b]
Vd_{ss} (ml/kg)	120 ± 18	89 ± 10	165 ± 38	115 ± 21
$AUC_{0-\infty}$ (μg·min/ml)	2720 ± 103	14031 ± 4496[b]	1862 ± 230[a]	8597 ± 2350[b]

[a] $P < 0.05$ compared with controls.
[b] $P < 0.05$ compared with its antipode.

of one-compartment model. Pharmacokinetic parameters were obtained by the nonlinear least square method using WinNonlin software (Pharsight, Mountain View, CA). Plasma concentration-time profiles of *S*-IB after intravenous administration of *S*-IB were fitted to the following equations:

$$V_{1(S)} \cdot \frac{dC_{1(S)}}{dt} = -\left(k_{10(S)} + k_{12(S)}\right) \cdot V_{1(S)} \cdot C_{1(S)} + k_{21(S)} \cdot X_{2(S)} \quad (1)$$

$$\frac{dX_{2(S)}}{dt} = k_{12(S)} \cdot X_{1(S)} - k_{21(S)} \cdot X_{2(S)} \quad (2)$$

where $C_{1(S)}$ is the plasma concentration of *S*-IB in the central compartment; $X_{1(S)}$ and $X_{2(S)}$ are the amounts of *S*-IB in the central and peripheral compartments, respectively; $V_{1(S)}$ is the volume of distribution of the central compartment; $k_{10(S)}$, $k_{12(S)}$, and $k_{21(S)}$ are the first-order rate constants as shown in Fig. 1.

Plasma concentration-time profiles of *R*-IB and *S*-IB after intravenous administration of *R*-IB were fitted to the following equations:

$$V_{1(R)} \cdot \left(dC_{1(R)}/dt\right) = -\left(k_{0(R)} + k_{12(R)} + k_{RS}\right) \cdot V_{1(R)} \cdot C_{1(R)} + k_{21(R)} \cdot X_{2(R)} \quad (3)$$

$$dX_{2(R)}/dt = k_{12(R)} \cdot X_{1(R)} - k_{21(R)} \cdot X_{2(R)} \quad (4)$$

$$V_{1(S)} \cdot \left(dC_{1(S)}/dt\right) = k_{RS} \cdot X_{1(R)} - \left(k_{10(S)} + k_{21(S)}\right) \cdot V_{1(S)} \cdot C_{1(S)} + k_{21(S)} \cdot X_{2(S)} \quad (5)$$

$$dX_{2(S)}/dt = k_{12(S)} \cdot X_{1(S)} - k_{21(S)} \cdot X_{2(S)} \quad (6)$$

where $C_{1(R)}$ is the plasma concentration of *R*-IB in the central compartment; $V_{1(R)}$ is the volume of distribution of the central compartment; $k_{10(R)} = k_{0(R)} + k_{RS}$, and $k_{0(R)}$, k_{RS}, $k_{12(R)}$, and $k_{21(R)}$ are the first-order rate constants as shown in Fig. 1. For the fitting of plasma concentration-time profiles of *S*-IB after intravenous administration of *R*-IB, parameter values obtained for *S*-IB after intravenous administration of *S*-IB were used for $V_{1(S)}$, $k_{10(S)}$, $k_{12(S)}$, and $k_{21(S)}$. Therefore, $V_{1(R)}$, $k_{10(R)}$, $k_{0(R)}$, k_{RS}, $k_{12(R)}$, and $k_{21(R)}$ were estimated from the fitting.

CL_{tot}, chiral inversion clearance (CL_{RS}), and metabolic clearance (CL_{MET}) were calculated using the following equations:

$$CL_{tot} = V_1 \times k_{10} \quad (7)$$

$$CL_{RS} = V_1 \times k_{RS} \quad (8)$$

$$R\text{-}IB;\ CL_{MET} = CL_{tot} - CL_{RS},\ S\text{-}IB;\ CL_{MET} = CL_{tot} \quad (9)$$

The fraction inverted from *R*-IB to *S*-IB after *R*-IB administration (Fi) was calculated using three approaches: the area under the plasma concentration-time curve (AUC) comparison, the deconvolution, and pharmacokinetic modeling methods. The fractional inversion using AUC (Fi_{AUC}) was calculated using the principles discussed by Pang and Kwan (1983) with the following equation:

$$Fi_{AUC} = \frac{AUC_{R \to S} \cdot \mathrm{Dose}_S}{AUC_{S \to S} \cdot \mathrm{Dose}_R} \quad (10)$$

where $AUC_{R \to S}$ is the $AUC_{0-\infty}$ of the metabolically formed *S*-IB after *R*-IB administration and $AUC_{S \to S}$ is the $AUC_{0-\infty}$ of *S*-IB after *S*-IB administration, assuming equal doses of *R*-IB and *S*-IB and no inversion from the *S*-IB to the *R*-IB (Adams et al., 1976; Hutt and Caldwell, 1983).

Determination of Protein Levels by Western Blot. Hepatic microsomes of control and AA rats were prepared according to a previously reported procedure (Iwaki et al., 1995; Nozaki et al., 2007). Sodium dodecyl sulfate-polyacrylamide gel electrophoresis was performed using 7.5% e-Pagell (Atto, Tokyo, Japan) and 50 μg microsome per well. Resolved proteins were transferred onto Hybond-P polyvinylidene difluoride membranes (GE Healthcare, Milwaukee, WI). Immunoreactive ACS1, APCE, and β-actin were detected using antibodies and an ECL Prime Western Blotting Detection system (GE Healthcare).

TABLE 2

Compartmental pharmacokinetic parameters of each enantiomer after intravenous administration of *rac*-IB

Results are expressed as the mean ± S.D. (n = 3).

Parameter	Control		AA	
	R-IB	*S*-IB	*R*-IB	*S*-IB
V_1 (ml/kg)	63.1 ± 4.4	67.3 ± 9.9	86.0 ± 34.2	95.8 ± 18.3
V_2 (ml/kg)	56.4 ± 24.6	56.0 ± 23.2	80.3 ± 28.4	68.3 ± 29.9
CL_{tot} (ml/min/kg)	4.01 ± 0.40	1.46 ± 0.40[b]	6.16 ± 1.11[a]	2.19 ± 0.67[b]
CL_{RS} (ml/min/kg)	2.75 ± 0.39	–	3.96 ± 0.67[a]	–
CL_{MET} (ml/min/kg)	1.26 ± 0.09	1.46 ± 0.40	2.19 ± 0.55[a]	2.19 ± 0.67
$k_{0(R)}$ (min^{-1})	0.020 ± 0.001	–	0.024 ± 0.007	–
k_{12} (min^{-1})	0.072 ± 0.031	0.070 ± 0.035	0.059 ± 0.030	0.070 ± 0.035
k_{21} (min^{-1})	0.074 ± 0.024	0.062 ± 0.020	0.076 ± 0.019	0.083 ± 0.018
k_{10} (min^{-1})	0.064 ± 0.007	0.021 ± 0.003[b]	0.076 ± 0.017	0.023 ± 0.004[b]
k_{RS} (min^{-1})	0.044 ± 0.007	–	0.052 ± 0.022	–

[a] $P < 0.05$ compared with controls.
[b] $P < 0.05$ compared with its antipode.
The em dashes indicate no value because of unidirectional chiral inversion of IB.

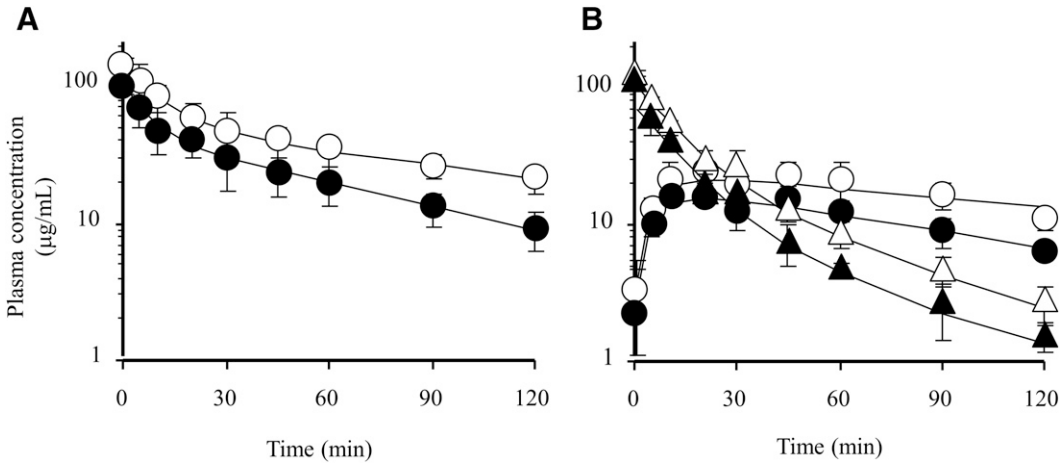

Fig. 3. Plasma concentration-time profiles of IB enantiomers after intravenous administration of *S*-IB (10 mg/kg) (A) or *R*-IB (10 mg/kg) (B) in control and AA rats. △, *R*-IB; ○, *S*-IB in control rat; ▲, *R*-IB; ●, *S*-IB in AA rats. Solid lines represent the fitting curves using the pharmacokinetic model shown in Fig. 1. Results are expressed as the mean ± S.D. (n = 3).

Statistical Analysis. The significant difference of the mean values between groups was estimated using analysis of variance followed by the Bonferroni test. A P value of <0.05 was considered statistically significant.

Results

The plasma concentration-time profiles of IB enantiomers after intravenous bolus injection of *rac*-IB (20 mg/kg) to control and AA rats were determined (Fig. 2). The plasma *R*-IB in both control and AA rats was rapidly eliminated. The plasma concentrations of both enantiomers in AA rats were slightly lower than corresponding antipodes in the controls. The noncompartmental pharmacokinetic parameters estimated from the results in Fig. 2 are summarized in Table 1. The stereoselective pharmacokinetics of IB were observed; for *R*-IB, relatively higher total clearance (CL_{tot}) and shorter mean residence time were observed compared with those of *S*-IB in both control and AA rats. There were no significant differences in distribution volumes at steady state (Vd_{ss}) between enantiomers, although the volumes of *R*-IB tended to be large. The CL_{tot} of each enantiomer was approximately 1.5 times increased in AA rats compared with that of control rats, although the increase in CL_{tot} of *S*-IB in AA rats was not significant.

To elucidate the effect of AA on the chiral inversion of *R*-IB to the *S*-antipode, compartment model analysis including the inversion process was performed. The pharmacokinetic parameters obtained from the model for each enantiomer of IB are summarized in Table 2. The distribution volume of the central compartment (V_1) and the peripheral compartment (V_2) of *R*-IB and *S*-IB in AA rats were slightly higher compared with those of the controls. There were no significant differences in metabolic clearance (CL_{MET}) between enantiomers in either control or AA rats. However, the CL_{tot} of *R*-IB was significantly higher than that of *S*-IB owing to the inversion of *R*-IB to *S*-IB. The inversion clearance (CL_{RS}) and CL_{MET} of *R*-IB increased in AA rats; the CL_{tot}, CL_{RS}, and CL_{MET} values were approximately 1.5 times higher in AA rats. On the other hand, there were no significant differences in CL_{tot} and CL_{MET} of *S*-IB between control and AA rats. Slight differences in $k_{0(R)}$, k_{12}, k_{21}, k_{10}, and k_{RS} were observed between control and AA rats. The inversion rate constants (k_{RS}) for *R*-IB in control and AA rats were 0.044 and 0.052 minute^{-1}, respectively, which accounted for approximately 70% of k_{10}.

To further clarify the effects of AA on the pharmacokinetics of each enantiomer, plasma concentration profiles of the IB enantiomers after the intravenous administration of either *R*-IB or *S*-IB were examined (Fig. 3). *R*-IB was not detected in plasma after *S*-IB administration, indicating that no or negligible inversion from *S*-IB to *R*-IB occurred in rats. *S*-IB was observed in plasma after *R*-IB administration, demonstrating the in vivo inversion of *R*-IB to *S*-IB. Plasma concentrations of *S*-IB increased up to approximately 20 minutes after the administration of *R*-IB. Subsequently, both *R*-IB and *S*-IB concentrations decreased and the concentrations of *S*-IB were higher than those of *R*-IB from approximately 30 minutes onward. The noncompartmental and compartmental pharmacokinetic parameters of *R*-IB and *S*-IB after intravenous administration of each enantiomer were estimated (Tables 3 and 4). The $T_{1/2}$ and Vd_{ss} for *R*-IB and *S*-IB did not change between control and AA rats. The CL_{tot} of *R*-IB and *S*-IB in AA rats significantly

TABLE 3

Noncompartmental pharmacokinetic parameters of each enantiomer after intravenous administration of *R*-IB or *S*-IB

Results are expressed as the mean ± S.D. (n = 3).

Parameter	Control			AA		
	R-IB after *R*-IB	*S*-IB after *R*-IB	*S*-IB after *S*-IB	*R*-IB after *R*-IB	*S*-IB after *R*-IB	*S*-IB after *S*-IB
$T_{1/2}$ (min)	33.9 ± 4.5	77.8 ± 24.4	84.2 ± 23.7[b]	30.4 ± 5.0	69.8 ± 23.9	56.3 ± 4.8[b]
CL_{tot} (ml/kg)	4.20 ± 0.23	–	1.30 ± 0.18[b]	6.20 ± 0.66[a]	–	2.40 ± 0.40[a,b]
MRT (min)	32.8 ± 5.4	–	109.3 ± 30.5[b]	26.7 ± 3.1	–	69.6 ± 8.77[a,b]
Vd_{ss} (ml/kg)	137 ± 18	–	146 ± 54	164 ± 10	–	168 ± 23
AUC (μg·min/ml)	2386 ± 129	3549 ± 474	7682 ± 1054[b]	1624 ± 171[a]	2090 ± 265a	4129 ± 568[a,b]

[a] $P < 0.05$ compared with controls.
[b] $P < 0.05$ compared with its antipode.
The em dashes indicate no value because of unidirectional chiral inversion of IB.

TABLE 4

Compartmental pharmacokinetic parameters of each enantiomer after intravenous administration of *R*-IB or *S*-IB

Results are expressed as the mean ± S.D. (n = 3).

Parameter	Control		AA	
	R-IB	*S*-IB	*R*-IB	*S*-IB
V_1 (ml/kg)	90.1 ± 20.0	67.2 ± 9.8	113 ± 38	99.3 ± 18.3
V_2 (ml/kg)	78.5 ± 29.2	93.4 ± 72.2	125 ± 52	112 ± 69
CL_{tot} (ml/min/kg)	4.28 ± 0.19	1.26 ± 0.12[b]	6.87 ± 1.05[a]	2.83 ± 0.92[a,b]
CL_{RS} (ml/min/kg)	2.21 ± 0.53	–	3.81 ± 0.42[a]	–
CL_{MET} (ml/min/kg)	2.07 ± 0.32	1.26 ± 0.12[b]	3.05 ± 0.42[a]	2.83 ± 0.92[a]
$k_{0(R)}$ (min^{-1})	0.023 ± 0.003	–	0.029 ± 0.009	–
k_{12} (min^{-1})	0.026 ± 0.018	0.056 ± 0.030	0.029 ± 0.010	0.058 ± 0.020
k_{21} (min^{-1})	0.031 ± 0.018	0.046 ± 0.020	0.033 ± 0.013	0.050 ± 0.017
k_{10} (min^{-1})	0.048 ± 0.008	0.019 ± 0.004[b]	0.060 ± 0.008	0.028 ± 0.006[b]
k_{RS} (min^{-1})	0.026 ± 0.011	–	0.032 ± 0.003	–

[a] $P < 0.05$ compared with controls.
[b] $P < 0.05$ compared with its antipode.
The em dashes indicate no value because of unidirectional chiral inversion of IB.

increased compared with those in control rats. The AUCs of each enantiomer after administration of the respective enantiomer and of *S*-IB after *R*-IB administration in AA rats significantly decreased compared with those in control rats. Table 4 demonstrates the tendency for V_1 and V_2 to be increased in AA rats after *rac*-IB administration. The CL_{tot} and CL_{MET} of *R*-IB and *S*-IB in AA rats significantly increased compared with those in control rats, the results being similar to those after intravenous administration of *rac*-IB. The fraction inverted from *R*-IB to *S*-IB after *R*-IB administration (*F*i) and the half-life for inversion ($T_{1/2inv}$) in control and AA rats were estimated using AUC analysis, deconvolution method, and model analysis (Table 5). The *F*i values of *R*-IB in both control and AA rats were approximately 50%, indicating that half of *R*-IB underwent chiral inversion to *S*-IB and that little difference in *F*i values was observed between control and AA rats.

The protein levels of ACS1 and APCE in hepatic microsomes of control and AA rats were determined (Fig. 4). ACS1 and APCE are involved in chiral inversion of IB. The protein levels of ACS1 were unchanged between control and AA rats. The significant decreases of APCE expression in AA rats were observed.

Metabolic enzyme activities and plasma protein binding are the most important determinants of the pharmacokinetics of 2-APA. To clarify whether AA affected metabolic enzyme activities, we measured the glucuronidation activities and P450 contents of rat liver microsomes (Table 6). The glucuronidation activities for *S*-IB were approximately three to four times higher than those for *R*-IB in control and AA rats. AA induction resulted in a significant decrease in glucuronidation activities and P450 contents for both *R*-IB and *S*-IB, suggesting that phase Ⅰ and Ⅱ metabolisms for IB were reduced in AA rats. Total protein and albumin concentrations and the plasma protein binding of *R*-IB and *S*-IB in control and AA rats were measured (Tables 7 and 8). Serum total protein and albumin concentrations in AA rats significantly decreased compared with those in control rats. In particular, the decreases in albumin concentrations in AA rats were marked (approximately 65% of control). Both in vitro and in vivo plasma unbound fractions (f_u) of both enantiomers of IB in AA rats increased approximately 2.5 times compared with those in controls, although f_u of *S*-IB was significantly greater than those of *R*-IB in both control and AA rats.

Discussion

In arthritis, P450 activities and plasma protein levels are decreased (Toda et al., 1994; Meunier and Verbeeck, 1999a; Kawase et al., 2013). In AA rats, used as a model of rheumatic arthritis, the pharmacokinetics of various drugs are affected, owing to the alterations in P450 activities and plasma protein levels (Walker et al., 1986; Pollock et al., 1989; Piquette-Miller and Jamali, 1992,1995; Meunier and Verbeeck, 1999b). For example, the CL_{tot} of the unbound form of ketoprofen significantly decreased in AA rats, whereas that of total (bound and unbound) ketoprofen was unchanged (Meunier and Verbeeck, 1999b). We also reported that CL_{tot} of flurbiprofen increased approximately twofold in AA rats (Nagao et al., 2003). In the present study, we examined the effects of AA on the stereoselective pharmacokinetics, especially on chiral inversion, of IB in rats.

In AA rats, CL_{tot} of IB significantly increased, although the glucuronidation activities for IB and P450 contents in liver microsomes decreased to approximately 50% and 70%, respectively; it is unclear whether AA affects the protein or activity of UGT and P450 isoforms. Probably, the increased CL_{tot} of IB was caused by the elevated levels of f_u of IB due to the decreased plasma albumin levels in AA rats (Tables 7 and 8). We previously demonstrated that the changed plasma protein

TABLE 5

*F*i and $T_{1/2inv}$ of inversion calculated by *AUC* analysis, deconvolution method, and model analysis in control and AA rats

Results are expressed as the mean ± S.D. (n = 3).

	Control			AA		
	AUC analysis (Fi_{AUC})[a]	Deconvolution method (Fi_{DECON})[b]	Model analysis (Fi_{COMP})[c]	*AUC* analysis (Fi_{AUC})[a]	Deconvolution method (Fi_{DECON})[b]	Model analysis (Fi_{COMP})[c]
*F*i	0.47 ± 0.07	0.51 ± 0.13	0.52 ± 0.12	0.51 ± 0.08	0.53 ± 0.18	0.56 ± 0.05
$T_{1/2inv}$ (min)	–	15.9 ± 4.4	29.7 ± 10.5	–	14.1 ± 3.4	25.8 ± 7.7

[a] $Fi_{AUC} = AUC_{R\rightarrow S}/AUC_{S\rightarrow S}$.
[b] Calculated using the deconvolution method.
[c] $Fi_{COMP} = k_{RS}/k_{0(R)} + k_{RS}$.
The em dashes indicate no value because of unidirectional chiral inversion of IB.

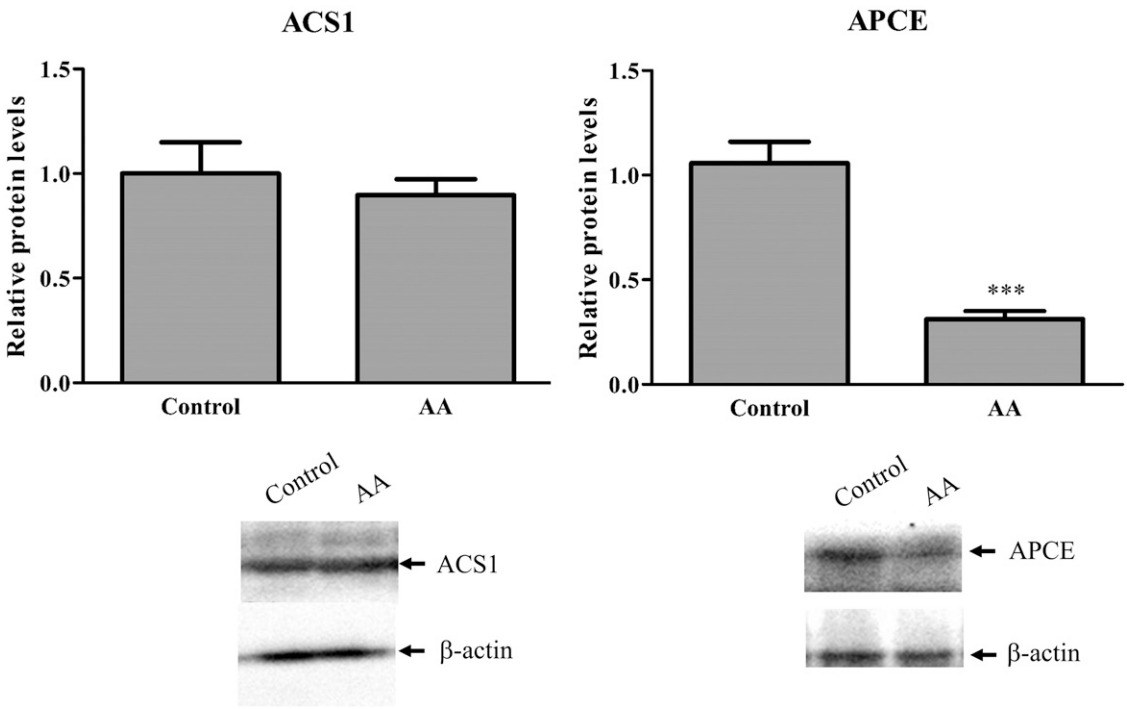

Fig. 4. Relative protein levels of ACS1 and APCE in hepatic microsomes of control and AA rats. Results are expressed as the mean ± S.D. (n = 5 or 6). Significant differences between control and AA rats are indicated. ***$P < 0.001$.

levels in AA rats leading to altered protein binding of drugs affect the pharmacokinetics of propranolol and flurbiprofen, which extensively bind to plasma protein under inflammatory conditions (Kawase et al., 2013). In humans, IB is also extensively (>98%) bound to albumin at therapeutic concentrations (Davies, 1998) and f_u of *S*-IB is twofold higher compared with that of *R*-IB, similar to the results in Table 8 (Evans et al., 1990; Tan et al., 2002). It is important to clarify the effects of AA on plasma levels of *S*-IB, because *S*-IB is involved in the expression of drug actions. In AA rats, decreased plasma levels of *S*-IB were observed after intravenous injection of *rac*-IB, *R*-IB, or *S*-IB compared with control rats (Figs. 2 and 3) without change of Fi and $T_{1/2inv}$, suggesting that drug actions of IB may be reduced in AA rats.

It is known that nonsteroidal anti-inflammatory drugs such as IB are conjugated in the liver to acyl glucuronides and excreted in bile (Mills et al., 1973). The efficiency of glucuronidation for *R*-IB or *S*-IB was suppressed in AA rats to 51% or 44% of control rats, respectively (Table 6). These results agreed with the report about ketoprofen by Meunier et al. (Meunier and Verbeeck, 1999b). The P450 contents in liver microsomes of AA rats significantly decreased by approximately 70% compared with that of control rats. Because most 2-APA including IB have relatively low levels of hepatic extraction, CL_{tot} of these drugs depends on both f_u and CL_{int}. IB is mainly metabolized by P450 and UGT (Hamman et al., 1997; Buchheit et al., 2011). The CL_{int} of AA rats could be decreased to approximately half the value of control rats because CL_{int} reflects the ability to eliminate the metabolized drug from the liver. Therefore, the increase of approximately 1.5 times in CL_{MET} of IB in AA rats after *rac*-IB administration could be a response to changes in f_u and CL_{int}, that is, in vivo plasma f_u of IB approximately 2.5 times (Table 8) and CL_{int} decreased by approximately half compared with that in control rats. Meunier and Verbeeck (1999b) showed that CL_{tot} of ketoprofen in AA rats did not significantly change. This result was interpreted as the approximately doubled f_u levels of ketoprofen negated the effect of decreased CL_{int} levels. The markedly elevated CL_{tot} of flurbiprofen in AA rats was assumed to be induced by the relatively higher protein-binding ratio of nonsteroidal anti-inflammatory drugs (Borgå and Borgå, 1997; Nagao et al., 2003). After intravenous administration of *R*-IB or *S*-IB, the effects of AA on CL_{tot}, CL_{RS}, and CL_{MET} of *S*-IB were larger compared with those of *R*-IB, although *rac*-IB exhibited similar effects of AA on CL_{tot} and CL_{MET} between *R*-IB and *S*-IB (Fig. 5). As these results demonstrate, there were some differences between the pharmacokinetics of each enantiomer of IB after intravenous administration of *rac*-IB and those after intravenous administration of *R*-IB or *S*-IB. Itoh et al. (1997) demonstrated that the enantiomer-enantiomer interaction in plasma protein binding affected the stereoselective pharmacokinetics of IB. Therefore, with intravenous

TABLE 6

Glucuronidation activities for *R*-IB and *S*-IB and P450 contents in control and AA rats

Results are expressed as the mean ± S.D. (n = 3).

		Control	AA
Glucuronidation activity (nmol/min/mg protein)	*R*-IB	0.23 ± 0.03	0.10 ± 0.01[a]
	S-IB	0.71 ± 0.07[b]	0.40 ± 0.04[a,b]
P450 contents (nmol/mg protein)		0.69 ± 0.10	0.48 ± 0.05[a]

[a]$P < 0.05$ compared with controls.
[b]$P < 0.05$ compared with its antipode.

TABLE 7

Plasma levels of total protein and albumin in control and AA rats

Results are expressed as the mean ± S.D. (n = 3).

	Control	AA
Total protein (g/dl)	6.9 ± 0.1	5.8 ± 0.1[a]
Albumin (g/dl)	2.7 ± 0.1	1.8 ± 0.1[a]

[a]$P < 0.05$ compared with controls.

TABLE 8

In vitro and in vivo plasma unbound fractions (f_u) (%) of IB in control and AA rats

Results are expressed as the mean ± S.D. (n = 3).

		Control		AA	
		R-IB	*S*-IB	*R*-IB	*S*-IB
In vitro		0.72 ± 0.24	1.38 ± 0.34	2.51 ± 0.56[b,c]	3.40 ± 0.57[b,c]
In vivo	Post dosing (min)				
	10	2.21 ± 0.32	2.96 ± 0.60	5.64 ± 0.66[b,c]	8.38 ± 3.18[b,c]
	30	2.16 ± 0.29	3.59 ± 0.53	5.81 ± 0.77[b,c]	7.42 ± 1.17[b,c]
	Average[a]	2.19	3.27	5.73	7.90

In vitro, *Rac*-IB (at a total concentration of 50 μg/ml); in vivo, dose, *rac*-IB 20 mg/kg. a) Average values between 10 and 30.
[b] $P < 0.05$ compared with controls.
[c] $P < 0.05$ compared with its antipode.

administration of *rac*-IB, it is necessary to consider the interactions between *R*-IB and *S*-IB in addition to the pharmacokinetics of each enantiomer.

The plasma concentrations of *S*-IB were significantly higher compared with those of *R*-IB after intravenous administration of *rac*-IB (Fig. 2). Similar stereoselective pharmacokinetics was observed for ketoprofen or fenoprofen (Rubin et al., 1985; Jamali and Brocks, 1990), suggesting that the higher CL_{tot} of *R*-IB compared with that of *S*-IB could be due to the process of chiral inversion in CL_{tot} of *R*-IB. Similar values for CL_{MET} between *R*-IB and *S*-IB were observed in control and AA rats (Table 2). The CL_{tot} of *S*-IB or *R*-IB could be expressed by the following equations:

$$CL_{tot(S)} = CL_{MET(S)} = f_{u(s)} \times CL_{int(S)} = f_{u(S)} \times \left(CL_{ox(S)} + CL_{glu(S)}\right) \quad (11)$$

$$CL_{tot(R)} = CL_{MET(R)} + CL_{RS} = f_{u(R)} \times CL_{int(R)} = f_{u(R)} \times \left(CL_{ox(R)} + CL_{glu(R)} + CL_{RS,int}\right) \quad (12)$$

CL_{ox} and CL_{glu} indicate the metabolic clearance of unbound IB for hydroxylation and glucuronidation, respectively. The following equation was derived from eq. 12.

$$CL_{MET(R)} = f_{u(R)} \times \left(CL_{ox(R)} + CL_{glu(R)}\right) \quad (13)$$

It is possible that the hydroxylation activity for *S*-IB was dominant compared with that of *R*-IB because similar values of CL_{MET} were exhibited despite the higher f_u and CL_{glu} of *S*-IB (Tables 6 and 8). Hamman et al. (1997) and Chang et al. (2008) showed the similar extents of stereoselective metabolisms of IB enantiomers by CYP2C. In in vivo study, P450-mediated clearance is more important for the *S*-IB (~70%) compared with the *R*-IB (~30%), because the unidirectional chiral inversion of *R*-IB to *S*-IB occurs (Rudy et al., 1991; Davies 1998). Glucuronidation activity for *S*-IB was 3 to 4 times higher than *R*-IB (Table 6), although the detailed mechanisms of preferential glucuronidation of *S*-IB is unclear. Our results concur with the report of el Mouelhi et al. (1987) that *S*-IB tends to convert to glucuronide compared with *R*-IB.

R-IB was undetectable in plasma after intravenous administration of *S*-IB (Fig. 3A), whereas *S*-IB was observed in plasma after intravenous administration of *R*-IB (Fig. 3B). These results were consistent with those of the studies by Knihinicki et al. (1991), Itoh et al. (1997), and Chen et al. (1991) on the unidirectional chiral inversion in rat. The *F*i of IB in control was about 50%, indicating that a half of *R*-IB underwent chiral inversion to *S*-IB. This result agreed with those of the studies by Knihinicki et al. (1991), Itoh et al. (1997), and Lee et al. (1984). Interestingly, little difference was observed between the *F*i and $T_{1/2inv}$ values of control and those of AA (Table 5). Chiral inversion comprises the following four steps (Knihinicki et al., 1989; Menzel et al., 1994): 1) the formation of *R*-ibuprofenyl-adenylate from *R*-IB, 2) the activation process from *R*-ibuprofenyl-adenylate to *R*-IB-CoA thioester by long-chain fatty acid ACS, 3) the racemization process of *R*-IB-CoA thioester by 2-aryl propionyl-CoA epimerase, and 4) the process of release of free IB by hydrolysis enzyme. APCE is present mainly in the liver and kidney (Shieh and Chen, 1993; Reichel et al., 1997). In inflammatory conditions, the activities of metabolic enzymes in the liver reduced as shown in this study (Table 6) and by other groups (Toda et al., 1994; Meunier and Verbeeck 1999a). However, in vivo efficiencies of chiral

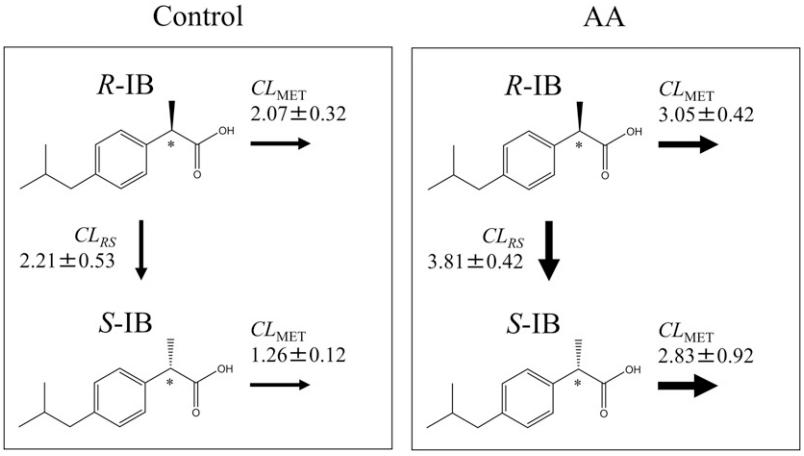

Fig. 5. Effects of AA induction on CL_{RS} (ml/min/kg) and CL_{MET} (ml/min/kg) of IB. Chiral centers indicated by an asterisk.

inversion of IB were not affected by AA. The protein levels of APCE1 but not ACS1 in AA rats significantly decreased compared with control rats (Fig. 4). These results suggested that the efficiencies of epimerization but not the formation of CoA thioester in chiral inversion from *R*-IB to *S*-IB could decrease in AA rats, if the protein binding (free fraction) is unchanged in AA rats. However, the decreased protein levels of APCE in AA rats have little effect on the chiral inversion ratio of IB, because the rate-limiting step in the chiral inversion of IB is CoA thioester formation but not epimerization and ibuprofenyl-CoA formation (Knihinicki et al., 1989; Knadler and Hall, 1990; Knights et al., 1991; Tracy and Hall, 1992). Few reports are available on the chiral inversion of *S*-IB to *R*-IB. The CL_{tot}, CL_{RS}, and CL_{MET} depend on both the metabolic activities and the protein binding of IB. The plasma unbound fraction of IB in AA rats was 2 to 3 times higher than that in control rats (Table 8). The glucuronidation activity and P450 contents in AA rats significantly decreased (Table 6). The P450 activities in AA rats also decreased, e.g., Cyp3a activities in AA rats reduced to approximately 20% of control (data not shown). As a cause of disagreements between the changes of CL and chiral inversion ratio in AA rats, there is a possibility that the decreased activities of P450, UGT, and enzymes catalyzing chiral inversion in AA rats are counterbalanced by the increased plasma free fraction of IB. Consequently, the ratios of chiral inversion were unchanged between control and AA rats. The effects of alterations in protein binding for IB on IB pharmacokinetics could possibly be larger than those in APCE activities in AA rats. Consequently, the ratios of chiral inversion could be unchanged between control and AA rats.

AA rats exhibit systemic inflammatory disease with changes to bone and cartilage similar to those observed in humans with rheumatoid arthritis (Williams, 1992). The effects of inflammation in arthritic patients on stereoselective pharmacokinetics is very interesting. However, it is unclear whether the human arthritis affects the stereoselective pharmacokinetics of 2-aryl propionic NSAIDs such as IB. A further study of changes of chiral inversion in arthritic patients should be conducted.

In conclusion, remarkable effects of AA on CL_{tot} of *S*-IB were observed compared with that of *R*-IB without changes in chiral inversion ratios from *R*-IB to *S*-IB after intravenous administration of *R*-IB or *S*-IB, although there were slight alterations in the effects of AA on CL_{tot} between stereoisomers after intravenous administration of *rac*-IB. These changes in the stereoselective pharmacokinetics of IB via decreased activity of P450 and UGT and elevated f_u could affect drug efficiencies.

Authorship Contributions

Participated in research design: Iwaki.
Conducted experiments: Ikuta and Kawase.
Performed data analysis: Ikuta and Kawase.
Wrote or contributed to the writing of the manuscript: Kawase and Iwaki.

References

Abas A and Meffin PJ (1987) Enantioselective disposition of 2-arylpropionic acid nonsteroidal anti-inflammatory drugs. IV. Ketoprofen disposition. *J Pharmacol Exp Ther* **240**:637–641.

Adams SS, Bresloff P, and Mason CG (1976) Pharmacological differences between the optical isomers of ibuprofen: evidence for metabolic inversion of the (-)-isomer. *J Pharm Pharmacol* **28**: 256–257.

Ahn HY, Amidon GL, and Smith DE (1991) Stereoselective systemic disposition of ibuprofen enantiomers in the dog. *Pharm Res* **8**:1186–1190.

Baillie TA, Adams WJ, Kaiser DG, Olanoff LS, Halstead GW, Harpootlian H, and Van Giessen GJ (1989) Mechanistic studies of the metabolic chiral inversion of (R)-ibuprofen in humans. *J Pharmacol Exp Ther* **249**:517–523.

Borgå O and Borgå B (1997) Serum protein binding of nonsteroidal antiinflammatory drugs: a comparative study. *J Pharmacokinet Biopharm* **25**:63–77.

Brocks DR and Jamali F (1994) Etodolac clinical pharmacokinetics. *Clin Pharmacokinet* **26**: 259–274.

Brune K, Geisslinger G, and Menzel-Soglowek S (1992) Pure enantiomers of 2-arylpropionic acids: tools in pain research and improved drugs in rheumatology. *J Clin Pharmacol* **32**: 944–952.

Buchheit D, Dragan CA, Schmitt EI, and Bureik M (2011) Production of ibuprofen acyl glucosides by human UGT2B7. *Drug Metab Dispos* **39**:2174–2181.

Caldwell J, Hutt AJ, and Fournel-Gigleux S (1988) The metabolic chiral inversion and dispositional enantioselectivity of the 2-arylpropionic acids and their biological consequences. *Biochem Pharmacol* **37**:105–114.

Castro EF, Soraci AL, Franci R, Fogel FA, and Tapia MO (2001) Disposition of suprofen enantiomers in the cat. *Vet J* **162**:38–43.

Chang SY, Li W, Traeger SC, Wang B, Cui D, Zhang H, Wen B, and Rodrigues AD (2008) Confirmation that cytochrome P450 2C8 (CYP2C8) plays a minor role in (S)-(+)- and (R)-(-)-ibuprofen hydroxylation in vitro. *Drug Metab Dispos* **36**:2513–2522.

Chen CS, Chen T, and Shieh WR (1990) Metabolic stereoisomeric inversion of 2-arylpropionic acids. On the mechanism of ibuprofen epimerization in rats. *Biochim Biophys Acta* **1033**:1–6.

Chen CS, Shieh WR, Lu PH, Harriman S, and Chen CY (1991) Metabolic stereoisomeric inversion of ibuprofen in mammals. *Biochim Biophys Acta* **1078**:411–417.

Davies NM (1995) Clinical pharmacokinetics of flurbiprofen and its enantiomers. *Clin Pharmacokinet* **28**:100–114.

Davies NM (1998) Clinical pharmacokinetics of ibuprofen. The first 30 years. *Clin Pharmacokinet* **34**:101–154.

Dietzel K, Beck WS, Schneider HT, Geisslinger G, and Brune K (1990) The biliary elimination and enterohepatic circulation of ibuprofen in rats. *Pharm Res* **7**:87–90.

el Mouelhi M, Ruelius HW, Fenselau C, and Dulik DM (1987) Species-dependent enantioselective glucuronidation of three 2-arylpropionic acids. Naproxen, ibuprofen, and benoxaprofen. *Drug Metab Dispos* **15**:767–772.

Evans AM, Nation RL, Sansom LN, Bochner F, and Somogyi AA (1990) The relationship between the pharmacokinetics of ibuprofen enantiomers and the dose of racemic ibuprofen in humans. *Biopharm Drug Dispos* **11**:507–518.

Foster RT, Jamali F, Russell AS, and Alballa SR (1988) Pharmacokinetics of ketoprofen enantiomers in healthy subjects following single and multiple doses. *J Pharm Sci* **77**:70–73.

Hamman MA, Thompson GA, and Hall SD (1997) Regioselective and stereoselective metabolism of ibuprofen by human cytochrome P450 2C. *Biochem Pharmacol* **54**:33–41.

Hutt AJ and Caldwell J (1983) The metabolic chiral inversion of 2-arylpropionic acids–a novel route with pharmacological consequences. *J Pharm Pharmacol* **35**:693–704.

Itoh T, Maruyama J, Tsuda Y, and Yamada H (1997) Stereoselective pharmacokinetics of ibuprofen in rats: effect of enantiomer-enantiomer interaction in plasma protein binding. *Chirality* **9**: 354–361.

Iwaki M, Bischer A, Nguyen AC, McDonagh AF, and Benet LZ (1995) Stereoselective disposition of naproxen glucuronide in the rat. *Drug Metab Dispos* **23**:1099–1103.

Jamali F, Berry BW, Tehrani MR, and Russell AS (1988) Stereoselective pharmacokinetics of flurbiprofen in humans and rats. *J Pharm Sci* **77**:666–669.

Jamali F and Brocks DR (1990) Clinical pharmacokinetics of ketoprofen and its enantiomers. *Clin Pharmacokinet* **19**:197–217.

Kaiser DG, Vangiessen GJ, Reischer RJ, and Wechter WJ (1976) Isomeric inversion of ibuprofen (R)-enantiomer in humans. *J Pharm Sci* **65**:269–273.

Kawase A, Tsunokuni Y, and Iwaki M (2007) Effects of alterations in CAR on bilirubin detoxification in mouse collagen-induced arthritis. *Drug Metab Dispos* **35**:256–261.

Kawase A, Ikuta H, Uno S, Yamamoto K, Akitsu N, Nagao T, and Iwaki M (2013) Alteration in plasma protein binding properties of propranolol and flurbiprofen during development of adjuvant-induced arthritis in rats. *Xenobiotica* **43**:246–252.

Kawase A, Norikane S, Okada A, Adachi M, Kato Y, and Iwaki M (2014) Distinct alterations in ATP-binding cassette transporter expression in liver, kidney, small intestine, and brain in adjuvant-induced arthritic rats. *J Pharm Sci* **103**:2556–2564.

Knadler MP and Hall SD (1990) Stereoselective arylpropionyl-CoA thioester formation in vitro. *Chirality* **2**:67–73.

Knights KM, Addinall TF, and Roberts BJ (1991) Enhanced chiral inversion of R-ibuprofen in liver from rats treated with clofibric acid. *Biochem Pharmacol* **41**:1775–1777.

Knihinicki RD, Williams KM, and Day RO (1989) Chiral inversion of 2-arylpropionic acid nonsteroidal anti-inflammatory drugs–1. In vitro studies of ibuprofen and flurbiprofen. *Biochem Pharmacol* **38**:4389–4395.

Knihinicki RD, Day RO, Graham GG, and Williams KM (1990) Stereoselective disposition of ibuprofen and flurbiprofen in rats. *Chirality* **2**:134–140.

Knihinicki RD, Day RO, and Williams KM (1991) Chiral inversion of 2-arylpropionic acid nonsteroidal anti-inflammatory drugs–II. Racemization and hydrolysis of (R)- and (S)-ibuprofen-CoA thioesters. *Biochem Pharmacol* **42**:1905–1911.

Lee EJ, Williams KM, Graham GG, Day RO, and Champion GD (1984) Liquid chromatographic determination and plasma concentration profile of optical isomers of ibuprofen in humans. *J Pharm Sci* **73**:1542–1544.

Menzel S, Waibel R, Brune K, and Geisslinger G (1994) Is the formation of R-ibuprofenyl-adenylate the first stereoselective step of chiral inversion? *Biochem Pharmacol* **48**: 1056–1058.

Meunier CJ and Verbeeck RK (1999a) Glucuronidation of R- and S-ketoprofen, acetaminophen, and diflunisal by liver microsomes of adjuvant-induced arthritic rats. *Drug Metab Dispos* **27**: 26–31.

Meunier CJ and Verbeeck RK (1999b) Glucuronidation kinetics of R,S-ketoprofen in adjuvant-induced arthritic rats. *Pharm Res* **16**:1081–1086.

Mills RF, Adams SS, Cliffe EE, Dickinson W, and Nicholson JS (1973) The metabolism of ibuprofen. *Xenobiotica* **3**:589–598.

Müller S, Mayer JM, Etter JC, and Testa B (1990) Metabolic chiral inversion of ibuprofen in isolated rat hepatocytes. *Chirality* **2**:74–78.

Nagao T, Tanino T, and Iwaki M (2003) Stereoselective pharmacokinetics of flurbiprofen and formation of covalent adducts with plasma protein in adjuvant-induced arthritic rats. *Chirality* **15**:423–428.

Nozaki Y, Kusuhara H, Kondo T, Iwaki M, Shiroyanagi Y, Nakayama H, Horita S, Nakazawa H, Okano T, and Sugiyama Y (2007) Species difference in the inhibitory effect of nonsteroidal anti-inflammatory drugs on the uptake of methotrexate by human kidney slices. *J Pharmacol Exp Ther* **322**:1162–1170.

Omura T and Sato R (1964) Carbon monoxide-binding pigment of liver microsomes. I: Evidence for its hemoprotein nature. *J Biol Chem* **239**:2370–2378.

Pang KS and Kwan KC (1983) A commentary: methods and assumptions in the kinetic estimation of metabolite formation. *Drug Metab Dispos* **11**:79–84.

Pedrazzini S, De Angelis M, Muciaccia WZ, Sacchi C, and Forgione A (1988) Stereochemical pharmacokinetics of the 2-arylpropionic acid non-steroidal antiinflammatory drug flunoxaprofen in rats and in man. *Arzneimittelforschung* **38**:1170–1175.
Piquette-Miller M and Jamali F (1992) Effect of adjuvant arthritis on the disposition of acebutolol enantiomers in rats. *Agents Actions* **37**:290–296.
Piquette-Miller M and Jamali F (1995) Influence of severity of inflammation on the disposition kinetics of propranolol enantiomers in ketoprofen-treated and untreated adjuvant arthritis. *Drug Metab Dispos* **23**:240–245.
Pollock SH, Matthews HW, and D'Souza MJ (1989) Pharmacokinetic analysis of cyclosporine in adjuvant arthritic rats. *Drug Metab Dispos* **17**:595–599.
Reichel C, Brugger R, Bang H, Geisslinger G, and Brune K (1997) Molecular cloning and expression of a 2-arylpropionyl-coenzyme A epimerase: a key enzyme in the inversion metabolism of ibuprofen. *Mol Pharmacol* **51**:576–582.
Rubin A, Knadler MP, Ho PPK, Bechtol LD, and Wolen RL (1985) Stereoselective inversion of (R)-fenoprofen to (S)-fenoprofen in humans. *J Pharm Sci* **74**:82–84.
Rudy AC, Knight PM, Brater DC, and Hall SD (1991) Stereoselective metabolism of ibuprofen in humans: administration of R-, S- and racemic ibuprofen. *J Pharmacol Exp Ther* **259**:1133–1139.
Shieh WR and Chen CS (1993) Purification and characterization of novel "2-arylpropionyl-CoA epimerases" from rat liver cytosol and mitochondria. *J Biol Chem* **268**:3487–3493.
Tan SC, Patel BK, Jackson SH, Swift CG, and Hutt AJ (2002) Stereoselectivity of ibuprofen metabolism and pharmacokinetics following the administration of the racemate to healthy volunteers. *Xenobiotica* **32**:683–697.
Toda A, Ishii N, Kihara T, Nagamatsu A, and Shimeno H (1994) Effect of adjuvant-induced arthritis on hepatic drug metabolism in rats. *Xenobiotica* **24**:603–611.
Tracy TS and Hall SD (1992) Metabolic inversion of (R)-ibuprofen. Epimerization and hydrolysis of ibuprofenyl-coenzyme A. *Drug Metab Dispos* **20**:322–327.
Uno S, Kawase A, Tsuji A, Tanino T, and Iwaki M (2007) Decreased intestinal CYP3A and P-glycoprotein activities in rats with adjuvant arthritis. *Drug Metab Pharmacokinet* **22**:313–321.
Uno S, Uraki M, Komura H, Ikuta H, Kawase A, and Iwaki M (2008) Impaired intrinsic chiral inversion activity of ibuprofen in rats with adjuvant-induced arthritis. *Xenobiotica* **38**: 1410–1421.
Uno S, Uraki M, Ito A, Shinozaki Y, Yamada A, Kawase A, and Iwaki M (2009) Changes in mRNA expression of ABC and SLC transporters in liver and intestines of the adjuvant-induced arthritis rat. *Biopharm Drug Dispos* **30**:49–54.
Walker KA, Barber HE, and Hawksworth GM (1986) Mechanism responsible for altered propranolol disposition in adjuvant-induced arthritis in the rat. *Drug Metab Dispos* **14**:482–486.
Williams RC, Jr (1992) Rheumatoid factors: historical perspective, origins and possible role in disease. *J Rheumatol Suppl* **32**:42–45.

Address correspondence to: Dr. Masahiro Iwaki, Department of Pharmacy, Faculty of Pharmacy, Kindai University, 3-4-1 Kowakae, Higashi-osaka, Osaka 577-8502, Japan. E-mail: iwaki@phar.kindai.ac.jp